

Microwave response of superconducting platelet crystals

Chien-Jang Wu and Tseung-Yuen Tseng

*Department of Electronics Engineering and Institute of Electronics, National Chiao-Tung University,
Hsinchu, Taiwan, Republic of China*

(Received 12 June 1995; revised manuscript received 21 September 1995)

A theoretical study of the microwave response of isotropic and anisotropic superconductors in the Meissner state is presented. We consider a superconducting thin platelet crystal oriented in a parallel field configuration. The linear response analysis is investigated on the basis of modified two-fluid models along with the diffusion equation. The BCS coherence effect for conventional superconductors and the anomalous peak in the loss for anisotropic high- T_c cuprates are considered. The microwave properties are analyzed by the derived dimensionless magnetic permeability. The results show that thin edges have essentially nothing to do with the microwave loss in isotropic superconductors and the simple slab geometry suffices in studying their microwave properties. As for the high- T_c superconductors, the anisotropic effect itself makes the thin edges crucial in determining the microwave loss. The calculated results qualitatively indicate some good consistence with the reported experimental data. The role of thin edges of the superconducting platelet crystal in the microwave response is therefore evidently clarified. [S0163-1829(96)03825-8]

I. INTRODUCTION

The fundamental properties of superconductors can be investigated by the measurement of the microwave surface impedance Z_s . With measured $Z_s = R_s + jX_s$, one readily has important information about the electron conduction mechanism. The surface resistance R_s is related to the microwave loss and proportional to the unpaired electron concentration. The measurement of the surface reactance X_s can be used to extract the penetration depth λ and has something to do with the paired electron density. The surface impedance in the local electrodynamics is described as

$$Z_s = \sqrt{j\omega\mu_0/\sigma}, \quad (1)$$

where σ is the complex conductivity of superconductors defined as $\sigma = \sigma_1 - j\sigma_2$, where σ_1 and σ_2 are the real and imaginary parts of the conductivity, respectively. This expression basically describes the intrinsic properties of bulk material and is derived under the assumption of a semi-infinite geometry.

However, in microwave measurements, a potential interest is the use of thin platelet crystals to extract some fundamental physics. In this geometry, sample dimensions may play an important role in studying the microwave loss especially for highly anisotropic high- T_c superconductors. The analysis of the microwave response of the platelet based on Eq. (1) may not sound so good because of its independence from sample dimensions. We then have reason to investigate the electromagnetic response by using some alternative such as the ac magnetic permeability $\mu = \mu_1 - j\mu_2$ or the equivalent magnetic susceptibility $\chi = \mu - 1$.

Many workers have experimentally and theoretically considered the ac, rf, or microwave response of thin platelet geometry or its extreme case, the slab geometry. For high-quality crystals of $\text{YBa}_2\text{Cu}_3\text{O}_{7-x}$ (YBCO), the microwave properties have been measured by Hardy *et al.*,¹ Shibauchi *et al.*,² and Zhang *et al.*³ A comprehensive collection of mea-

surements of the surface impedance of high- T_c superconductors can be found in the paper of Müller *et al.*^{4,5} Most workers have usually fitted experimental results by using a two-fluid model with some variable parameters. Their results in general supported the validity of two-fluid theory even though it is intuitive and empirical. However, the microwave analysis from the expression of Z_s described above does not include sample dimensions and anisotropic properties explicitly. It therefore needs further theoretical analysis to examine the geometric effect on microwave properties. In this paper, we present a theoretical study on the microwave response of the platelet crystal. We carefully take into account the effect of sample dimensions from the field distribution inside the material. Our derivations will be made under the assumption of the linear and isotropic superconductors which are analyzed based on a modified two-fluid model.^{6,7} Regarding the highly anisotropic superconductors, the microwave response will be examined within the framework of the anisotropic linear resistive model.⁸

II. THEORETICAL CONSIDERATIONS

In describing the microwave response, one usually relies on the traditional two-fluid model (TTF), which was developed by Gorter and Casimir⁹ and then extended by London.¹⁰ This phenomenological model addresses microwave loss by including two noninteracting fluids, the normal electrons and superconducting electrons. The total electron concentration n consists of normal electron concentration n_n and super-electron concentration n_s , namely, $n = n_n + n_s$, and are given by¹¹

$$\eta_s \equiv n_s/n = 1 - t^4, \quad (2)$$

$$\eta_n \equiv n_n/n = t^4, \quad (3)$$

where t is the reduced temperature defined as $t = T/T_c$ and T_c is the transition temperature of the superconductor. In the microwave frequencies the electrodynamics of superconduct-

ors can be well described by this model as well as Drude theory. The normal-fluid conduction current density \mathbf{J}_n and supercarrier current density \mathbf{J}_s are given by

$$\mathbf{J}_n = \frac{\sigma'_n}{1 + j\omega\tau} \mathbf{E} = \sigma_1 \mathbf{E}, \quad (4)$$

$$\mathbf{E} = \mu_0 \lambda^2 \frac{\partial \mathbf{J}_s}{\partial t}, \quad (5)$$

$$\mathbf{B} = -\mu_0 \lambda^2 \nabla \times \mathbf{J}_s, \quad (6)$$

where $\sigma'_n = \sigma_n \eta_n$, with σ_n the dc normal-state conductivity, τ is the momentum relaxation time of normal electrons, \mathbf{E} is the electric field, \mathbf{B} is the magnetic flux density, μ_0 is the permeability of free space, and λ is the London penetration depth given as $\lambda(t) = \lambda(0)(1 - t^4)^{-1/2}$. Combining with Maxwell's equation

$$\nabla \times \mathbf{H} = \nabla \times (\mathbf{B}/\mu_0) = \mathbf{J}_n + \mathbf{J}_s = \mathbf{J} \quad (7)$$

and the fact that $\omega\tau \ll 1$, we have the magnetic flux diffusion equation

$$\left(1 - \lambda^2 \nabla^2 + \mu_0 \sigma'_n \lambda^2 \frac{\partial}{\partial t}\right) \mathbf{H} = 0. \quad (8)$$

This equation is valid for a linear isotropic superconductor and able to describe the electrodynamic response if the magnetic field within the material can be found.

The TTF model accurately predicts the frequency dependence of microwave loss (the surface resistance R_s is proportional to ω^2), even its intuitive nature, but it fails to correctly describe the dependences of microwave loss on temperature T , penetration depth λ and microscopic parameters, the coherence length ξ_0 , and electron mean free path l . For the case of conventional BCS superconductors, it has been shown that the electromagnetic response is related to the coherence effect, the microscopically quantum mechanical result. In high-temperature superconductors, the temperature dependence of the microwave surface resistance indicates the existence of a nearly temperature-independent residual resistance at lower temperatures.⁷ The TTF model, however, is unable to explain both the coherence factor in BCS superconductors and the residual resistance in high- T_c oxides. These may be considered as the key defects of the TTF model.

Recently, a fast and accurate fit for the BCS coherence effect within the framework of the two-fluid model, called the modified two-fluid (MTF) model, has been developed by Linden *et al.*,⁶ who used a BCS conductivity program by Zimmermann *et al.*¹² They extracted the real part of complex conductivity and assumed the validity of Drude theory of conduction electrons. A good fit for the BCS coherence factor included in two-fluid theory was found. The fraction of normal-fluid electrons is given by

$$\eta_n(\omega, T) = \frac{2\Delta(T)}{k_B T} \exp\left(-\frac{\Delta(T)}{k_B T}\right) \ln\left(\frac{\Delta(T)}{\hbar \omega_1}\right) \times \left[\frac{a'}{1 + (\omega/\omega_0)^{b'}} + c' \right], \quad (9)$$

where the gap energy $\Delta(T)$ of the BCS superconductor is approximated by

$$\Delta(T) \approx \Delta(0) \left[\cos\left(\frac{\pi}{2} t^2\right) \right]^{1/2},$$

k_B is the Boltzmann constant, \hbar the Planck constant, $\omega_1 = 1$ rad/sec, and the parameters a' , b' , c' , and ω_0 depend on the ratio l/ξ_0 . For typical BCS strong coupling superconductors, Nb ($T_c = 9.2$ K), whose $l = 100$ nm, $\xi_0 = 39$ nm, we find that $a' = 0.31$, $b' = 0.474$, $c' = 0$, and $\omega_0 = 25$ GHz.⁶ These parameters will be used in the later part of this paper.

As far as the residual surface resistance in high- T_c oxides is concerned, many workers have proposed models to interpret the measured residual loss. Müller *et al.*⁷ have introduced a modified two-fluid model to explain the surface impedance of high- T_c superconductors. They introduced an additional component of the nonpairing charge carrier n_{res} , which is assumed to be weakly temperature dependent. Based on this n_{res} , it consequently introduces a corresponding residual real part of the complex conductivity, namely, σ_{res} . The residual surface resistance R_{res} is found to be proportional to $\omega^2 \lambda^3 \sigma_{\text{res}}$ according to the two-fluid model. However, experimental analysis on their model has not been carried out. Kobayashi and Imai¹³ later treated the nonpairing residual normal electron n_{res} as the third fluid and proposed a phenomenologically so-called three-fluid model to investigate the surface impedance of high- T_c YBCO bulk plates successfully. In one of their papers,¹⁴ the real part of the conductivity σ_1 has been fitted as

$$\sigma_1 = \sigma'_n = \sigma_n t^4 + \sigma_{\text{res}}, \quad (10)$$

with $\sigma_n = 3.67 \times 10^5$ S/m and $\sigma_{\text{res}} = 1 \times 10^5$ S/m for YBCO plates at 10.4 GHz. While the imaginary part of conductivity σ_2 was kept as usual according to the TTF model, the result was

$$\sigma_2 = (\omega \mu_0 \lambda^2)^{-1} = (1 - t^4) [\omega \mu_0 \lambda^2(0)]^{-1}. \quad (11)$$

Recently, Bonn *et al.*¹⁵ have also proposed a generalized two-fluid model in dealing with the residual loss in the surface resistance of their measurements of very-high-quality YBCO platelets. They modeled the normal fluid fraction $\eta_n(t)$ as

$$\eta_n(t) = t^2 [1 - \eta_n(0)] + \eta_n(0), \quad (12)$$

where $\eta_n(0)$ is a sample-dependent residual normal fluid and it is assumed that the residual normal fluid has the same momentum relaxation time as the intrinsic normal fluid.

Much effort has been made in dealing with the residual loss of high- T_c cuprates, and the influence of material anisotropy on microwave surface impedance has rarely been examined. More recently, many workers have switched their

attention to the anisotropic effect on the microwave properties especially for single-crystal platelets.¹⁶⁻¹⁹ We are here in a position to interpret the anomalous peak¹⁶ in microwave loss in the extremely anisotropic superconductor, Bi-2212 [Bi₂Sn₂CaCu₂O₈ (BSCCO)]. To theoretically study the microwave response, we shall use the anisotropic linear resistive model instead of the two-fluid model. The application of the resistive model here is based on two reasons. One is that the superconductor can be essentially regarded as a normal conductor.⁸ The other is that the anisotropic diffusion equation based on the anisotropic two-fluid model is still not available to date to our knowledge. The components of the resistivity tensor in the superconducting state used in the resistive model are assumed to follow Arrhenius behavior, namely, the thermally assisted type. The Meissner-state resistivity can be empirically expressed as^{8,20,27}

$$\rho = \rho_0 \exp(-C/k_B T), \quad (13)$$

where the prefactor ρ_0 and constant C are fitting constants which will be described later. By the way, in the thermally assisted flux flow regime, the prefactor ρ_0 is independent of the field and orientation applied, whereas C is the activation energy related to the dc magnetic field and temperature. In this paper, we are only concerned with the Meissner response at zero field. No flux lines are introduced, and the resistivity basically has nothing to do with the activation energy.

III. DERIVATIONS OF DIMENSIONLESS MAGNETIC AC PERMEABILITY

A. Isotropic superconductors

We consider a long thin superconducting platelet with length $2b$, width $2a$, and thickness $2c$. We assume that $2b \gg 2a \gg 2c$ for the purpose of neglecting the demagnetization factor. A \hat{z} -polarized microwave field $h_0 e^{j\omega t}$ is applied parallel to the main flat surfaces. Figure 1 depicts the cross section ($2a \times 2c$) of a thin platelet crystal. It is worth mentioning that the coordinate in Fig. 1 has the same corresponding crystallographic axes in high- T_c superconductors. To calculate the microwave absorption of this thin platelet, we first consider the extreme case of slab geometry with thickness $2c$. We are only interested in the field penetrations through two main flat surfaces. We treat the superconductor as a linear system, and the response is obtained first by considering an applied unit step field $u(t)$ at time $t < 0$, where $u(t)$ is expressed as

$$u(t) = \begin{cases} 1, & t \leq 0, \\ 0, & t > 0. \end{cases} \quad (14)$$

Therefore, the initial field distribution inside the slab at time $t=0$ can be written as a form of Fourier expansion,

$$h_u(x,0) = 1 - \frac{4}{\pi} \sum_{n=0}^{\infty} \frac{(-1)^n \cos[(2n+1)(\pi/2c)x]}{2n+1}. \quad (15)$$

The field gradually penetrates into the slab from the surface at time $t > 0$; the field distribution will be the form of

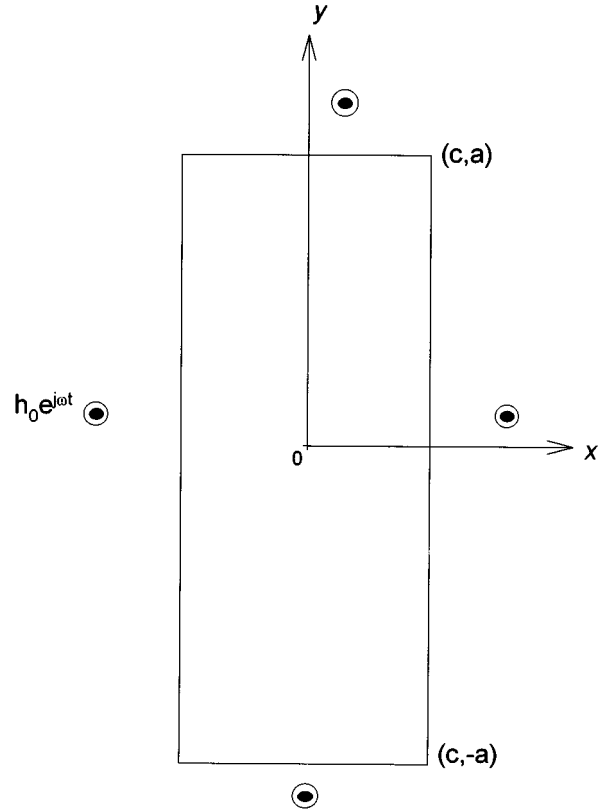


FIG. 1. Cross section of a thin platelet, where the x - z plane corresponds to the Cu-O a - b plane and the \hat{y} direction is the crystallographic c axis. The \hat{z} direction is perpendicular to the paper plane. The \hat{z} -polarized microwave field $h_0 e^{j\omega t}$ is applied along the \hat{z} direction.

$$h_u(x,t) = 1 - \frac{4}{\pi} \sum_{n=0}^{\infty} \frac{(-1)^n \cos[(2n+1)(\pi/2c)x]}{2n+1} e^{-K_n t}, \quad (16)$$

where the penetration rate $1/K_n$ can be found from the magnetic diffusion equation, Eq. (8). The result is

$$K_n = \tau_0^{-1} \left[1 + \lambda^2 \left(\frac{(2n+1)\pi}{2c} \right)^2 \right], \quad (17)$$

with $\tau_0 \equiv \mu_0 \sigma_n' \lambda^2$. Following a similar procedure to that in the study of Gough and Exon,¹⁶ we have the impulse response

$$h_i(x,t) = \frac{4}{\pi} \sum_{n=0}^{\infty} \frac{(-1)^n K_n \cos[(2n+1)(\pi/2c)x]}{2n+1} e^{-K_n t} \quad (18)$$

and the linear ac (microwave) response

$$H(x,t) = \frac{4h_0}{\pi} \sum_{n=0}^{\infty} \frac{(-1)^n \cos[(2n+1)(\pi/2c)x]}{2n+1} \times \frac{K_n}{K_n + j\omega} e^{j\omega t}. \quad (19)$$

Then for effective dimensionless magnetic ac permeability, $\mu = \mu_1 - j\mu_2$ is directly calculated as

$$\mu_{\text{slab}} = \frac{8}{\pi^2} \sum_{m=\text{odd}} \frac{1}{m^2} \frac{K_m}{K_m + j\omega}, \quad (20)$$

where K_m is described in Eq. (17) and is now rewritten as $K_m = \tau_0^{-1} + \alpha^2 m^2$, with $\alpha^2 = \pi^2 \tau_0^{-1} (\lambda/2c)^2$, and m is a positive odd number. Equation (20) is further evaluated in the Appendix; the analytic result is

$$\mu_{\text{slab}} = \frac{1}{1 + j\omega\tau_0} + \frac{j\omega\tau_0}{1 + j\omega\tau_0} \frac{\tan[(c/\lambda)\sqrt{-(1 + j\omega\tau_0)}]}{(c/\lambda)\sqrt{-(1 + j\omega\tau_0)}}. \quad (21)$$

The corresponding effective surface impedance Z_s can be obtained from the power relation; one has

$$H(x, y, t) = \frac{16h_0}{\pi^2} \sum_{m,n=0}^{\infty} \frac{(-1)^{m+n} K_{mn}}{K_{mn} + j\omega} \frac{\cos[(2m+1)(\pi/2c)x] \cos[(2n+1)(\pi/2a)y]}{(2m+1)(2n+1)} e^{j\omega t}. \quad (23)$$

The effective dimensionless magnetic ac permeability can be calculated as follows:

$$\mu_{\text{rect}} = \frac{64}{\pi^4} \sum_{p,q} \frac{1}{p^2 q^2} \frac{K_{pq}}{K_{pq} + j\omega}, \quad (24)$$

where p, q are positive odd numbers and K_{pq} is expressed as

$$\begin{aligned} K_{pq} &= \tau_0^{-1} \left\{ 1 + \lambda^2 \left[\left(p \frac{\pi}{2c} \right)^2 + \left(q \frac{\pi}{2a} \right)^2 \right] \right\} \\ &= \tau_0^{-1} + \alpha^2 p^2 + \beta^2 q^2. \end{aligned}$$

In the Appendix, we further calculate Eq. (24) in a more analytical form; the result is

$$\begin{aligned} \mu_{\text{rect}} &= \frac{1}{1 + j\omega\tau_0} - \frac{1}{1 + j\omega\tau_0} \frac{\tan[(\pi/2)x]}{(\pi/2)x} \\ &+ \frac{16}{\pi^3} \sum_p \left[\frac{\tan[(\pi/2)x_p]}{p^2 x_p} + \frac{\tan[(\pi/2)y_p]}{p^2 y_p} \right. \\ &\left. - \frac{1}{1 + j\omega\tau_0 + \alpha^2 \tau_0 p^2} \frac{\tan[(\pi/2)y_p]}{p^2 y_p} \right], \quad (25) \end{aligned}$$

where

$$-x_p^2 = \tau_0^{-1} \alpha^{-2} + \beta^2 \alpha^{-2} p^2 + j\omega \alpha^{-2},$$

$$-y_p^2 = \tau_0^{-1} \beta^{-2} + \alpha^2 \beta^{-2} p^2 + j\omega \beta^{-2},$$

$$-x^2 = \tau_0^{-1} \alpha^{-2} + j\omega \alpha^{-2},$$

$$\alpha^2 = \pi^2 \tau_0^{-1} (\lambda/2c)^2,$$

$$\beta^2 = \pi^2 \tau_0^{-1} (\lambda/2a)^2,$$

and

$$Z_s = \frac{1}{2} j\omega \mu_0 2c \mu_{\text{slab}}. \quad (22)$$

It is evident that Z_s is thickness dependent and essentially quite different from the surface impedance described in Eq. (1) previously. However, in theoretical investigations of microwave response, one usually has only to consider the ac magnetic permeability for convenience.

In the above derivation, we have found the ac permeability for slab geometry. We go on to extend it to the rectangular rod with cross section $2a \times 2c$; namely, the field penetrations by four planes parallel to the microwave field are considered. As analogous derivation for slab geometry, the linear microwave response $H(x, y, t)$ is consequently calculated easily, and the result is

$$\tau_0 = \mu_0 \sigma_n' \lambda^2 = \mu_0 \sigma_n \eta_n \lambda^2.$$

Clearly, the permeability of the rectangular rod described in Eq. (25) depends on the sample dimensions, temperature, and operating frequency and is complicated explicitly. The series in Eq. (25) are convergent rapidly and can be calculated by computer program. We will show the numerical results later. Besides, it is worthy to note that Eq. (25) can reproduce the μ_{slab} in Eq. (21) for both slabs with thickness $2c$ and $2a$ if one let $2a \rightarrow \infty$ and $2c \rightarrow \infty$, respectively. Therefore, Eq. (25) is indeed a general expression of the ac permeability for rectangular rods.

B. Anisotropic superconductors

Consider now the anisotropic rectangular rod in the same configuration; the microwave response is examined with the help of the anisotropic linear resistivity model. The magnetic diffusion equation is

$$\left(\rho_c \frac{\partial^2}{\partial x^2} + \rho_a \frac{\partial^2}{\partial y^2} \right) H = \mu_0 \frac{\partial H}{\partial t}. \quad (26)$$

Assuming the temporal part as $e^{j\omega t}$ and by matching the boundary conditions at $x = \pm a$, $y = \pm c$, the solution of Eq. (26) can be directly obtained. The result is

$$\begin{aligned} H(x, y, t) &= \sum_{n=0}^{\infty} (-1)^n \frac{2h_0}{\alpha_n} \left[\cos\left(\frac{\alpha_n}{\alpha} x\right) \frac{\cosh(k_y y)}{\cosh(k_y c)} \right. \\ &\left. + \cos\left(\frac{\alpha_n}{c} y\right) \frac{\cosh(k_x x)}{\cosh(k_x a)} \right] e^{j\omega t}, \quad (27) \end{aligned}$$

where

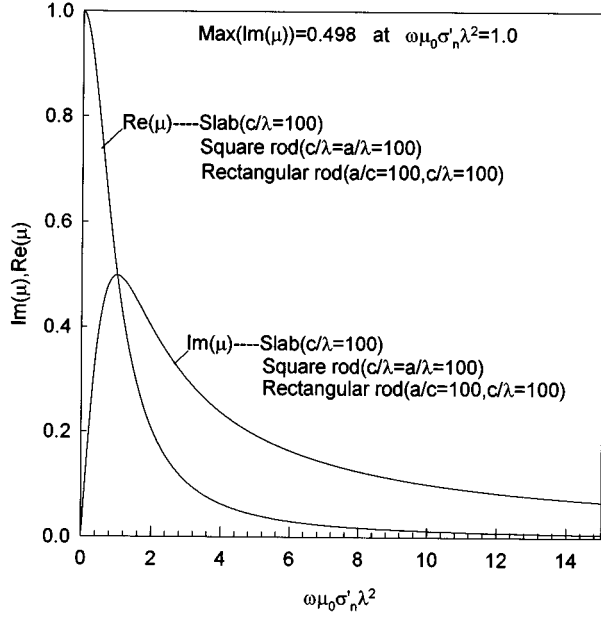


FIG. 2. Imaginary and real components in Eqs. (21) and (25) as a function of $\omega\mu_0\sigma_n'\lambda^2$ for three illustrated geometries. The slab is chosen with a half-thickness $c=100\lambda$ and rectangular rod with aspect ratio $a/c=100$ and $c=100\lambda$. The square rod is taken as $a=c=100\lambda$.

$$\alpha_n = \left(n + \frac{1}{2}\right)\pi, \quad n=0,1,2,\dots,$$

$$k_x = (\rho_c/\rho_a)^{1/4} \sqrt{k^2 + (\rho_c/\rho_a)^{1/2}(\alpha_n/a)^2},$$

$$k_y = (\rho_a/\rho_c)^{1/4} \sqrt{k^2 + (\rho_a/\rho_c)^{1/2}(\alpha_n/c)^2},$$

$$k = j\omega\mu_0/\sqrt{\rho_a\rho_c}.$$

The corresponding effective magnetic permeability is

$$\mu_{\text{rect}} = \sum_{n=0}^{\infty} \frac{2}{\alpha_n^2} \left[\frac{\tanh(k_x a)}{k_x a} + \frac{\tanh(k_y c)}{k_y c} \right]. \quad (28)$$

Equation (28) will be applied to investigate the extreme anisotropic high- T_c superconductor, the BSCCO system, if the Arrhenius resistivities are fed in.

The result in Eq. (28) appears to be more compact than that provided by Gough and Exon [Eq. (15) in Ref. 16] and can reproduce the same results shown in their study.²¹ Our derivation here in Eq. (27) is just like the problem of solving standard Helmholtz equation [Eq. (26)] with some boundary conditions, while the previous results, Eqs. (19) and (23), in the isotropic case as well as that provided by Gough and Exon¹⁶ were obtained based on the assumption of a linear system. In a linear system, the ac response can be obtained from the integration of the impulse response as described in Sec. III A.

IV. RESULTS AND DISCUSSION

To investigate the microwave loss of the isotropic platelet crystal, we first consider the permeabilities of slab in Eq. (21) and rectangular rod in Eq. (25). Figure 2 illustrates the

real and imaginary components of μ for three different geometries as a function of $\omega\tau_0 = \omega\mu_0\sigma_n'\lambda^2$. The slab is taken with half-thickness equal to 100λ , the thin rectangular rod with a ratio of width to thickness, a/c , equal to 100 (with $c=100\lambda$), and a square rod with $a=c=100\lambda$. The results show a striking feature; namely, the overall behaviors of these three geometries are identical. This feature can be qualitatively argued as follows. First, assuming the field penetration through two thin edges surfaces is not considered, we only consider the field penetration through two main flat planes, that is, the slab one. Introducing the field penetration immediately through two thin edges will consequently enhance the loss of the platelet. However, on the other hand, these field penetrations will reduce the gradient of the field originally penetrating through main planes. The reduction of the gradient of the magnetic field will consequently yield a decrease in the current density from Ampère's law. This results in a decrease of the microwave loss. The amount of decreasing loss is expected to be equal to the increasing loss originally generated from thin edges. The resultant effect on loss from four planes is identical to the slab one. We thus are tempted to conclude that the losses from thin edges may be neglected; namely, the slab geometry will suffice in investigating the microwave loss for thin platelets in the parallel field configuration. The same argument also holds good even for a square rod as can be observed in Fig. 2. The above argument may be concluded from the feature of isotropy in λ of superconductors.

The above result is quite different from the microwave response of an Ohmic (resistive) anisotropic superconductor. In a highly anisotropic high- T_c superconductors such as Bi-2212, the normal-state microwave response¹⁶ has elucidated the importance of the thin edges. Indeed, in anisotropic superconductors the thin edges play a crucial role in microwave properties; it has been shown that the amount of decreased loss by the reduction of the gradient of the magnetic flux through the main planes is greater than the increased loss from field penetrations through thin edges because of the strong anisotropy in skin depths. The result leads to a reduction in microwave loss. The Meissner-state microwave response of very anisotropic superconductors will be considered later.

Another feature shown in Fig. 2 is the existence of a peak in the imaginary part of the permeability with a value of about 0.498. This peak loss occurs at $\omega\mu_0\sigma_n'\lambda^2=1$. However, for conventional superconductors in the microwave region, the value of $\omega\mu_0\sigma_n'\lambda^2$ at $T < T_c$ is always much less than unity. Therefore, the overall loss lies in the region of $\omega\mu_0\sigma_n'\lambda^2 < 1$ Fig. 2 and increases with increasing temperature or increases with increasing frequency. It is therefore not expected to observe the loss peak in the microwave regime. In weakly anisotropic superconductors such as YBCO, if we approximate it as an isotropic one, one would not either observe the existence of the loss peak. This inexistence of the peak loss is consistent with experimental data based on measurements of microwave surface resistances.^{4,6} The measured surface resistance in general drops rapidly below T_c and behaves nearly linear with frequency. The extremely anisotropic high- T_c superconductor Bi-2212, however, shows a loss peak near T_c .¹⁶ This peak in surface resistance has been

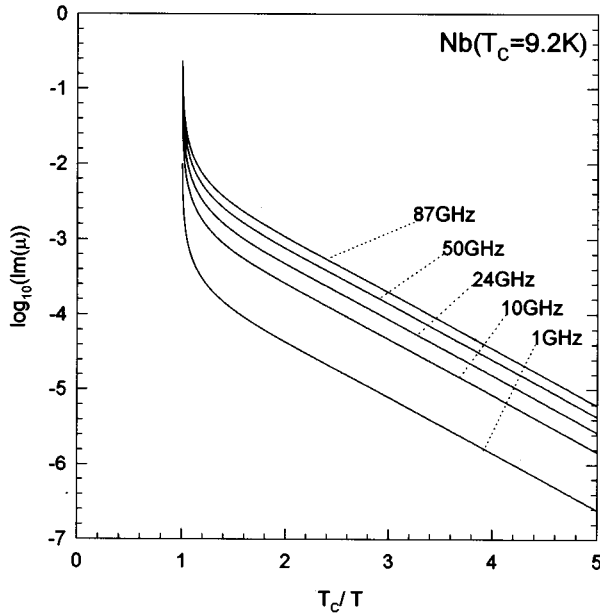


FIG. 3. Imaginary part of permeability as a function of temperature based on Eq. (21) for a conventional superconductor Nb ($T_c=9.2$ K) at various frequencies. Parameters are $\lambda(0)=40$ nm, $\sigma_0=3.2\times 10^6$ S/m, $l=10$ nm, $\xi_0=39$ nm, and $2c=1$ mm.

ascribed to the skin size effect from thin edges, which is closely related to the large anisotropy in resistivity.¹⁶ In principle, if one has an anisotropic diffusion equation similar to Eq. (8), one can transform it to an isotropic one by suitable scaling. The loss peak will be possibly expected. This possibility may be attributed to the very large penetration depth in strongly anisotropic high- T_c cuprates, which will cause the value of $\omega\mu_0\sigma_n'\lambda^2$ to be larger than unity. We later will deal with this question theoretically and give a good interpretation of the anomalous loss peak near T_c .

We now turn our attention to the application of Eq. (21) in conventional BCS superconductors such as Nb ($T_c=9.2$ K). A comparison will be made between our results and the reported experimental data. For a strong coupling BCS superconductor Nb, the coherence effect is reflected in the modification of the fraction of normal electrons, η_n , as described in Eq. (9), the MTF model. The temperature-dependent penetration depth of the strong coupling superconductor is approximated by $\lambda(T)=\lambda(0)[1-(T/T_c)^4]^{-1/2}$, and the gap energy $\Delta(T)$ is

$$\Delta^2(T)\approx\Delta^2(0)\left[\cos\left(\frac{\pi}{2}(T/T_c)^2\right)\right],$$

with $\Delta(0)=1.97k_B T_c$. By taking $\lambda(0)=40$ nm, $l=100$ nm, $\xi_0=39$ nm, $\sigma_n=3.2\times 10^6$ S/m, and $2c=1$ mm, the temperature- and frequency-dependent imaginary parts of the permeability are illustrated in Figs. 3 and 4, respectively. Figure 3 indicates that the overall loss decreases with decreasing temperature and exhibits a sharp transition at T_c . Meanwhile, the higher the frequency, the larger the loss at $T<T_c$. The behavior in Fig. 3 shows good agreement with microwave measurements on the surface resistance.⁵ In the measured surface resistance for conventional superconductors, it has been observed that R_s drops sharply at T_c followed

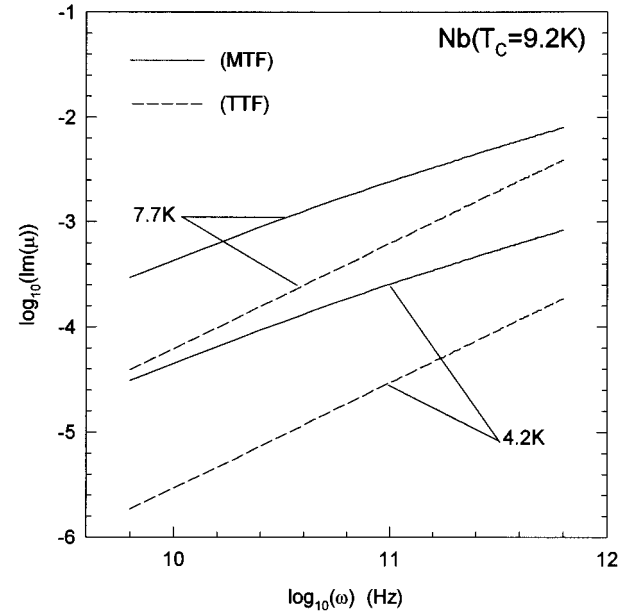


FIG. 4. Frequency dependence of the imaginary part of the permeability at $T=4.2$ and 7.7 K based on Eq. (21). The results are compared by using the TTF and MTF models. The linear frequency is varied from 1 to 100 GHz. Parameters are $\lambda(0)=40$ nm, $\sigma_0=3.2\times 10^6$ S/m, $l=100$ nm, $\xi_0=39$ nm, and $2c=1$ mm.

by an exponential decrease at temperatures $T<0.8T_c$. This is also shown in the imaginary part of the permeability, μ_2 , in Fig. 3. In Fig. 4, the frequency-dependent losses at 4.2 and 7.7 K are shown according to the TTF (dashed line) and MTF (solid line) models. It clearly elucidates the enhancement of loss which results from the inclusion of the coherence factor. Besides, the deviation of the linear relation with frequency at higher frequency is also obviously observed. This again agrees with the reported data about microwave surface resistance.^{5,6} The frequency-dependent R_s based on the TTF model is predicted to be linear (in log-log scale), which is only valid for lower frequency. This linear relation is a result of a first-order approximation with the fact that for $\sigma_2\gg\sigma_1$ even T is near T_c and describes the measured R_s well at low frequency. However, as for the measured R_s at higher frequency, the linear relation clearly fails. This can be remedied by the MTF model or by the general relations between R_s , σ_1 , and σ_2 , which can be found in Ref. 5. Figure 4 clearly demonstrates the deviation of the linear relation at higher frequency as expected in R_s . The difference between the MTF and TTF models shown in Fig. 4 decreases with increasing frequency. At low frequency, this difference is larger when the temperature is low, while at high frequency the difference becomes small as temperature is high. This comparison of the MTF and TTF models on the frequency dependence on loss is generally in accordance with that predicted by Linden *et al.*⁶ This loss predicted by the MTF model is now shown more compatible with experimental results. In BCS theory, the coherence effect produces a peak in the real component of the ac conductivity, which can be argued as an increase in the normal-fluid density just below T_c followed by an exponential decrease at lower temperatures. As a matter of fact, the coherence effect in superconductors originates from the dynamic properties of the

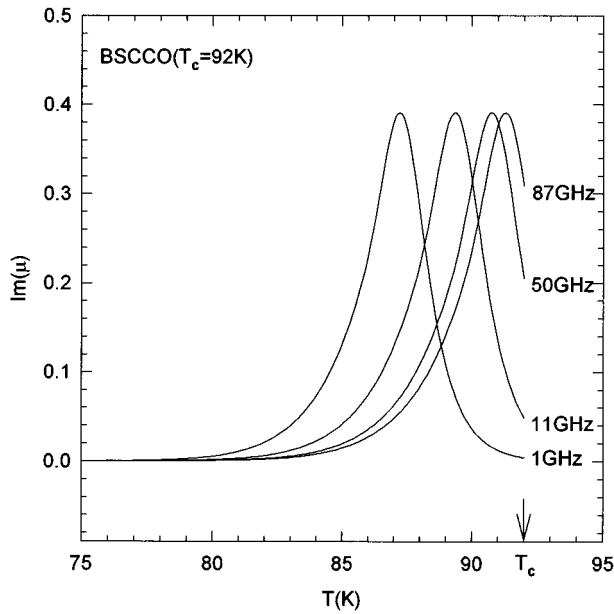


FIG. 5. Temperature dependence of the imaginary part of the permeability in Eq. (28) at various frequencies for a BSCCO platelet. Parameters are $2a=1$ mm, $2c=10$ μm , $T_c=92$ K, $\rho_a=1.65\times 10^{35}\exp(-175/0.02T)$, and $\rho_c=2.5\times 10^{40}\exp(-175/0.02T)$.

quasiparticle excitations which differ from those of normal electron-hole excitations as the gap develops at $T < T_c$. A good interpretation of the conductivity of BCS superconductors on the basis of the two-fluid framework can be found in the paper of Berlinsky *et al.*²² In high- T_c cuprates, the real part of the ac conductivity σ_1 also exhibits a coherence peak in the superconducting state.^{23–25} However, the nature of peak in σ_1 in high- T_c oxides is understood in the framework of the marginal Fermi-liquid theory; namely, the inelastic-scattering rate plays a vital role in σ_1 . At $T < T_c$, it has been argued that the strong reduction in the inelastic-scattering rate causes the peak in σ_1 instead of the interference of the wave functions of a Cooper pair. This coherence peak in conductivity of course has a salient influence on the microwave response, as can be seen in Ref. 26. This phenomenon is beyond the scope of two-fluid theory; we will therefore not try to investigate it in this paper.

As a final discussion, we focus on the application of Eq. (28) to the extremely anisotropic high- T_c superconductor, the BSCCO system. The temperature-dependent microwave losses are shown in Fig. 5 at different frequencies. The thickness $2c=10$ μm , width $2a=1$ mm, and the material parameters $T_c=92$ K, and Arrhenius-type resistivities $\rho_a=1.65\times 10^{35}\exp(-175/0.02T)$ Ωm , $\rho_c=2.5\times 10^{40}\exp(-175/0.02T)$ Ωm in zero field are taken to simulate the microwave response. The resistivities here are obtained from the experimental measurements at $B=0$ as reported in the works of Palstra *et al.*²⁰ and Exon *et al.*²⁷ Let us compare the results in Fig. 5 with the reported data. First, the anomalous peak near T_c in the zero-field surface resistance shown in Ref. 16 is evidently observed from the imaginary part of the permeability. Additionally, this peak can be attributed to the field penetration through edge surfaces due to the large anisotropy in resistivities (ρ_c/ρ_a about 10^5). At the

frequency of 11 GHz, the peak loss occurs at $T\approx 89$ K, which corresponds to a skin depth of $\delta_a\approx 0.35$ mm and $\delta_c\approx 1$ μm . Therefore, the field penetration through thin edges is heavily large because the δ_a is comparable with the half width (0.5 mm), which is in agreement with the argument provided by Gough and Exon.¹⁶ We therefore conclude that the anomalous peak in R_s is due to the skin size effect. Second, the peak will shift to lower temperature as decreasing the microwave frequency, which is consistent with ac permeability data of Palstra *et al.*²⁰ The appearance of a loss peak in Fig. 5 is easily expected at lower frequency. At frequencies higher than 90 GHz, the peak disappears and the loss shows a monotonous decrease at $T < T_c$. At temperatures lower than about 80 K, the losses coalesce to zero for all frequencies. Attention is now turned to the YBCO system. In this weakly anisotropic high- T_c compound, the resistivity anisotropy ρ_c/ρ_a is reported to be not larger than 10 according to the work of Palstra *et al.*²⁰ With this small anisotropy (compared with BSCCO), the field penetration through thin edges is no longer as heavy as BSCCO. The skin size effect described above is therefore not expected. The anomalous peak loss near T_c shown in BSCCO is consequently disappeared in YBCO, which is in agreement with reported surface resistance data.^{15,17} The application of the anisotropic linear resistive model in YBCO, however, is only reasonably good in the temperature regime near T_c ; namely, the imaginary part of permeability drops abruptly just below T_c . The low-temperature behavior is unfortunately not described well in this model. In recent reports of the surface resistances of high-quality YBCO single crystals, a small peak around 35 K was observed by Anlage *et al.*¹⁷ and Bonn *et al.*¹⁵ Moreover, a linear temperature-dependent R_s below 20 K and larger residual resistance are also observed by Anlage *et al.*¹⁷ The surface resistance in the low-temperature regime is possibly related to a sample imperfection, that is, strongly material dependent. The nature of these peculiar behaviors should closely correlate with the mechanism of superconductivity. It is therefore suggested that the theoretical approach to the microwave response of YBCO needs further consideration and investigation. As far as the role of thin edges in YBCO crystals is concerned, it is tempting to conclude that the effect of thin edges should not be as salient as BSCCO.

We have systematically analyzed the microwave losses of isotropic and anisotropic superconductors in the parallel field configuration on the basis of the results of our derivations. The theoretical results sound good in comparing with the reported experimental data. We thus believe that the microwave response of isotropic superconductors can be theoretically investigated well within the framework of a modified two-fluid picture and the validity of the resistive model in explaining the highly anisotropic superconductors is also verified.

V. CONCLUSIONS

The microwave properties of superconducting thin platelets have been investigated in the present study. According to the diffusion equation combined with the modified two-fluid model and anisotropic linear resistive model, some important conclusions can be drawn as follows.

(1) An alternative for analyzing the microwave response can be well described by the derived magnetic ac permeability which includes the sample dimensions.

(2) We have shown that the microwave properties can be simply investigated in the shape of slab geometry for the isotropic superconducting platelet crystal in the parallel field configuration. It means that the microwave absorption is entirely determined by the main flat surfaces instead of the thin edges. However, the thin edges play a crucial role in determining the microwave losses for highly anisotropic superconductors.

(3) In the isotropic superconductors such as BCS conventional ones, the inclusion of a coherence factor in our derivation has reasonably elucidated the consistence between our results and the reported experimental data.

(4) For strongly anisotropic high- T_c superconductors such as BSCCO, a possible analysis can be made by the anisotropic linear resistive model together with anisotropic Arrhenius resistivities.

ACKNOWLEDGMENT

This work is supported by the National Science Council of R.O.C. under Project No. NSC 84-2112-M009-026.

APPENDIX

Let us consider Eq. (20); we now rewrite it for convenience as follows:

$$\mu_{\text{slab}} = \frac{8}{\pi^2} \sum_{m=\text{odd}} \frac{1}{m^2} \frac{K_m}{K_m + j\omega}, \quad (\text{A1})$$

where

$$K_m = \tau_0^{-1} + \alpha^2 m^2. \quad (\text{A2})$$

Substituting (A2) into (A1) and after some manipulation, one easily has

$$\mu_{\text{slab}} = \frac{8}{\pi^2} \sum_{m=\text{odd}} \left[\frac{(1+j\omega\tau_0)^{-1}}{m^2} + \frac{1}{m^2-x^2} - \frac{(1+j\omega\tau_0)^{-1}}{m^2-x^2} \right], \quad (\text{A3})$$

where $-x^2 = \alpha^{-2}\tau_0^{-1} + j\omega\alpha^{-2}$.

The last two summations can be evaluated by a residue integral.¹⁶ The result is

$$\mu_{\text{slab}} = \frac{j\omega\tau_0}{1+j\omega\tau_0} \frac{\tan[(\pi/2)x]}{\frac{\pi}{2}x} + \frac{1}{1+j\omega\tau_0}. \quad (\text{A4})$$

This is exactly the same as Eq. (21) if the explicit form of x is fed into (A4).

Similarly, Eq. (24) can be rewritten now as

$$\mu_{\text{rect}} = \frac{64}{\pi^4} \sum_{p,q} \frac{1}{p^2 q^2} \frac{K_{pq}}{K_{pq} + j\omega}, \quad (\text{A5})$$

where

$$K_{pq} = \tau_0^{-1} + \alpha^2 p^2 + \beta^2 q^2. \quad (\text{A6})$$

By feeding (A6) into (A5), one can decompose it as

$$\mu_{\text{rect}} = \frac{64}{\pi^4} \sum_{p,q} \left[\frac{\tau_0^{-1}}{p^2 q^2 (\tau_0^{-1} + \alpha^2 p^2 + \beta^2 q^2 + j\omega)} + \frac{\alpha^2}{q^2 (\tau_0^{-1} + \alpha^2 p^2 + \beta^2 q^2 + j\omega)} + \frac{\beta^2}{p^2 (\tau_0^{-1} + \alpha^2 p^2 + \beta^2 q^2 + j\omega)} \right]. \quad (\text{A7})$$

The first series in (A7) can then be calculated directly; the result is

$$\sum_{p,q} \frac{\tau_0^{-1}}{p^2 q^2 (\tau_0^{-1} + \alpha^2 p^2 + \beta^2 q^2 + j\omega)} = \frac{\pi^4}{64} \frac{1}{1+j\omega\tau_0} - \frac{\pi^3}{32} \frac{1}{1+j\omega\tau_0} \frac{\tan[(\pi/2)x]}{x} - \frac{\pi}{4} \sum_p \frac{1}{1+j\omega\tau_0 + \alpha^2 \tau_0 p^2} \frac{\tan[(\pi/2)y_p]}{p^2 y_p}, \quad (\text{A8})$$

where $-y_p^2 = \alpha^2 \beta^{-2} p^2 + \beta^{-2} \tau_0^{-1} + j\omega \beta^{-2}$.

The second series and third one in (A7) are also evaluated easily; the results are

$$\sum_{p,q} \frac{\alpha^2}{q^2 (\tau_0^{-1} + \alpha^2 p^2 + \beta^2 q^2 + j\omega)} = \frac{\pi}{4} \sum_p \frac{\tan[(\pi/2)x_p]}{p^2 x_p}, \quad (\text{A9})$$

where $-x_p^2 = \beta^2 \alpha^{-2} p^2 + \alpha^{-2} \tau_0^{-1} + j\omega \alpha^{-2}$ and

$$\sum_{p,q} \frac{\beta^2}{p^2 (\tau_0^{-1} + \alpha^2 p^2 + \beta^2 q^2 + j\omega)} = \frac{\pi}{4} \sum_p \frac{\tan[(\pi/2)y_p]}{p^2 y_p}. \quad (\text{A10})$$

On the basis of (A8), (A9), and (A10), we finally have the permeability of the rectangular rod expressed as Eq. (25).

¹W. N. Hardy, D. A. Bonn, D. C. Morgan, Ruixing Liang, and Kuan Zhang, Phys. Rev. Lett. **70**, 3999 (1993).

²T. Shibauchi, H. Kitano, A. Maeda, T. Tamegai, K. Uchinokura, T. Kimura, K. Kishio, H. Asaoka, and H. Takei, Physica C **235-240**, 1819 (1994).

³K. Zhang, D. A. Bonn, Ruixing Liang, D. J. Barr, and W. N. Hardy, Appl. Phys. Lett. **62**, 3019 (1993).

⁴G. Müller, D. J. Brauer, R. Eujen, M. Hein, N. Klein, H. Piel, L. Ponto, U. Klein, and M. Peiniger, IEEE Trans. Magn. **MAG-25**, 2402 (1989).

⁵H. Piel and G. Muller, IEEE Trans. Magn. **MAG-27**, 854 (1991).

⁶D. S. Linden, T. P. Orlando, and W. G. Lyons, IEEE Trans. Appl. Supercond. **AS-4**, 136 (1994).

⁷G. Muller, N. Klein, A. Brust, H. Chaloupka, M. Hein, S. Orbach,

- H. Piel, and D. Reschke, *J. Supercond.* **3**, 235 (1990).
- ⁸R. Busch, G. Ries, H. Werthner, G. Kreiselmeyer, and G. Saemann-Ischenko, *Phys. Rev. Lett.* **69**, 522 (1992).
- ⁹C. J. Gorter and H. G. B. Casimir, *Phys. Z.* **35**, 963 (1934).
- ¹⁰H. London, *Proc. R. Soc. London A* **176**, 522 (1940).
- ¹¹T. V. Duzer and C. W. Turner, *Principles of Superconductive Devices and Circuits* (Elsevier, New York, 1981).
- ¹²W. Zimmermann, E. H. Brandt, M. Bauer, E. Seider, and L. Genzel, *Physica C* **183**, 99 (1991).
- ¹³Y. Kobayashi and T. Imai, *IEICE Trans. Commun. E* **74**, 1986 (1991).
- ¹⁴Y. Kobayashi, T. Imai, and H. Kayano, *IEEE Trans. Microwave Theory Tech.* **MTT-39**, 1530 (1991).
- ¹⁵D. A. Bonn, R. Liang, T. M. Riseman, D. J. Baar, D. C. Morgan, K. Zhang, P. Dosanjh, T. L. Duty, A. MacFarlane, G. D. Morris, J. H. Brewer, W. N. Hardy, C. Kallin, and A. J. Berlinsky, *Phys. Rev. B* **47**, 11 314 (1993).
- ¹⁶C. E. Gough and N. J. Exon, *Phys. Rev. B* **50**, 488 (1994).
- ¹⁷S. M. Anlage, D. H. Wu, J. Mao, S. N. Mao, X. X. Xi, T. Venkatesan, J. L. Peng, and R. L. Greene, *Phys. Rev. B* **50**, 523 (1994).
- ¹⁸K. Zhang, D. A. Bonn, S. Kamal, R. Liang, D. J. Baar, W. N. Hardy, D. Bosov, and T. Timusk, *Phys. Rev. Lett.* **73**, 2484 (1994).
- ¹⁹J. Mao, D. H. Wu, J. L. Peng, R. L. Greene, and S. M. Anlage, *Phys. Rev. B* **51**, 3316 (1995).
- ²⁰T. T. M. Palstra, B. Batlogg, R. B. van Dover, L. F. Schneemeyer, and J. V. Waszczak, *Phys. Rev. B* **41**, 6621 (1990).
- ²¹C. J. Wu and T. Y. Tseng, *Phys. Rev. B* **54**, 665 (1996).
- ²²A. J. Berlinsky, C. Kalin, G. Rose, and A. C. Shi, *Phys. Rev. B* **48**, 4074 (1993).
- ²³M. C. Nuss, P. M. Mankiewich, M. L. O'Malley, and E. H. Westerwick, *Phys. Rev. Lett.* **66**, 3305 (1991).
- ²⁴D. B. Romero, C. D. Porter, D. B. Tanner, L. Forro, D. Mandrus, L. Mihaly, G. L. Carr, and G. P. Williams, *Phys. Rev. Lett.* **68**, 1590 (1992).
- ²⁵D. A. Bonn, P. Dosanjh, R. Liang, and W. N. Hardy, *Phys. Rev. Lett.* **68**, 2390 (1992).
- ²⁶G. Grüner, in *Phenomenology and Applications of High Temperature Superconductors*, edited by K. S. Bedell *et al.* (Addison-Wesley, Reading, MA, 1992), p. 77.
- ²⁷N. Exon, M. Lancaster, A. Porch, G. Yang, and C. E. Gough, *IEEE Trans. Appl. Supercond.* **AS-3**, 1442 (1993).